

ELECTRON BEAM SIZE AND PROFILE MEASUREMENTS WITH REFRACTIVE X-RAY LENSES

T. Weitkamp, O. Chubar, M. Drakopoulos, I. Snigireva, A. Snigirev, ESRF, Grenoble, France
C. Schroer, F. Guenzler, B. Lengeler, RWTH, Aachen, Germany

Abstract

An application of compound refractive lenses (CRL) with parabolic shape of holes for electron beam size and profile measurements with hard X-rays is described. A CRL optimised for the radiation of 8 – 30 keV photon energy is an excellent tool for the imaging of electron beam in high-energy electron storage rings. Optical resolution of the imaging scheme based on such lens (estimated as full width at half-maximum of the transfer function) can be as small as 4 – 10 microns. This is smaller than typical values of vertical size of electron beam in synchrotron sources of the third generation. The results of measurements at two ESRF beamlines and the resolution calculations taking into account the features of synchrotron radiation and transmission characteristics of the CRL are presented.

1 INTRODUCTION

Recent advances in the development of Compound Refractive Lenses (CRLs) for hard X-rays have brought about robust devices that can be used for the focusing of high-energy synchrotron radiation (SR) and, since recently, as imaging tools [1,2]. Among the advantages of CRLs over other imaging lenses for the hard X-rays, such as Fresnel zone plates, are ease of alignment, variability of the focal length, and a robust design that allows exposure to high heat load without damage to the lens.

With the development of parabolic CRLs, which have no spherical aberrations, high-quality imaging with hard X-rays became available. A hard X-ray microscope using a CRL objective has been shown to work and is now used at the ESRF beamline ID-22 [2].

We present here the electron beam imaging experiments carried out at two ESRF beamlines - a bending magnet and an undulator beamline - using different detection methods.

2 IMAGING SETUP

At the bending-magnet BM-5, where the first experiment was carried out, the beamline geometry (one long combined optical/experimental hutch and another experimental hutch further downstream) gives access to the X-ray beam at the positions allowing a 1:1 imaging (the source-to-lens and lens-to-image distances L_1 and L_2 are equal, $L_1 = L_2 = 2f$, and the image has the same size as the source). The experiment was carried out at a photon

energy of 8.9 keV, i.e., in the lower range of energies typically used with CRLs. Only a single refractive lens with a focal length of $f = 13.6$ m was used. The detection system consisted of a small aperture, i.e. a pinhole with a diameter of $5 \mu\text{m}$, that was raster-scanned over the image plane, and a scintillation counter positioned behind the pinhole. Fig. 1-A shows the setup schematically.

The second experiment was carried out at the undulator beamline ID-18, at a photon energy of 23 keV and using a CRL made of 7 single lenses. The focal length of the CRL was $f = 13.6$ m and the distances were $L_1 = 40.4$ m and $L_2 = 19.5$ m, i.e., the image was demagnified by a factor of $L_1/L_2 = 2.09$. Another method was used for image detection: a gold knife edge was scanned through the image plane and the fluorescence signal from the Au L_α line was measured by a Si-Li detector that remained fixed in space (Fig. 1-B). A derivative of the signal as a function of the edge position gives a profile of the image along the direction of the scan. This technique does not yield a full image, but it ensures higher detector resolution required for the demagnified imaging geometry.

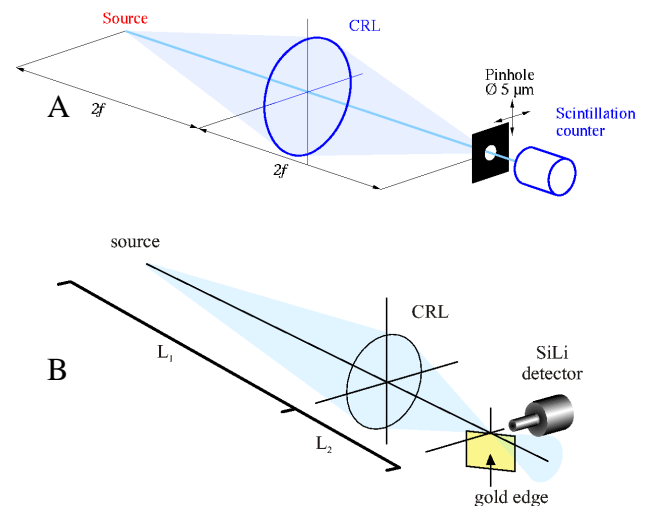


Figure 1. Experiment setup.

A: Bending-magnet beamline BM-5. A small aperture is raster-scanned over the image plane. The full image of the source is recorded as mesh data with an NaI scintillation counter behind the aperture.

B: Undulator beamline ID-18. A gold knife edge is scanned through the image plane and the fluorescence signal is detected by a Silicon-Lithium detector that remains fixed in space.

3 RESOLUTION CALCULATIONS

To estimate the optical resolution of electron beam transverse size and profile measurements with CRLs, we computed the intensity distribution in the image plane that one would observe for a single electron (or a “filament” electron beam). The computation was done in two steps. First, the transverse electric field of synchrotron radiation was computed at the longitudinal position of the CRL. The computation was performed using the retarded potentials method [4]:

$$\vec{E} = iek \int_{-\infty}^{+\infty} [\vec{\beta} - \vec{n} [1 + i(kr)^{-1}]] r^{-1} \exp[ik(c\tau + r)] d\tau \quad (1)$$

where k is the radiation wave number, $\vec{\beta} = \vec{\beta}(\tau)$ instant relative velocity of electron, $\vec{n} = \vec{n}(\tau)$ unit vector directed from instant electron position to an observation point, $r = r(\tau)$ distance from the electron to the observation point, c the speed of light, e the charge of electron.

Next, the electric field was propagated, using the methods of Fourier optics, through parabolic CRL and a drift space, from the plane immediately after the CRL, to the image plane. The propagation through the CRL was simulated by multiplication of the electric field by the complex transmission function of transverse position $T(x, y)$, that takes into account both the phase shift and attenuation of the electric field:

$$T(x, y) = \exp[-N(2l)^{-1} + ik\delta][d + p(x, y)] \quad (2)$$

$$p(x, y) = R^{-1} \times \begin{cases} x^2 + y^2, & x^2 + y^2 < R_0^2 \\ R_0^2, & x^2 + y^2 \geq R_0^2 \end{cases}$$

where R is the minimal radius of the lens surface curvature, R_0 is the radius of the aperture, δ the refraction index decrement, l the intensity attenuation length of the lens material, N the number of individual lenses in the CRL. The propagation through the drift space to the image plane was computed from the Huygens-Fresnel principle (using the convolution theorem and 2d FFT):

$$\vec{E}_{\perp}^*(x^*, y^*) \approx \frac{k}{2\pi i L} \iint \vec{E}_{\perp}(x, y) T(x, y) \times \exp[ik[L^2 + (x^* - x)^2 + (y^* - y)^2]^{1/2}] dx dy \quad (3)$$

where L is distance from the lens to the image plane, \vec{E}_{\perp} is transverse electric field obtained from Eq. (1), \vec{E}_{\perp}^* the transverse electric field in the image plane.

The computed single-electron intensity distributions in the plane before the lens, immediately after the lens, and in the image plane, are shown in Fig. 2. The computation was performed for the two different cases, for which the experiments were carried-out: the bending magnet SR (magnetic field of 0.85 T) at 8.9 keV photon energy, and the undulator radiation (UR) from a 38 x 42 mm undulator at 23 keV photon energy. The electron beam energy in the two cases was 6 GeV. The geometrical aperture of the

CRL was 0.89 mm, the lens surface was a paraboloid of rotation, with minimal radius of 190 μm .

The computed FWHM sizes of the single-electron intensity distributions in the image plane are: 7.3 μm for 8.9 keV bending magnet SR, and 4.1 μm for 23 keV UR (see lower right graph in Fig. 2). These values can be used as estimations of optical resolution in assumption of perfect focusing surfaces of the CRLs.

One can see from Fig. 2 that in the case of bending-magnet SR (upper and lower plots), the resolution is limited by the effective CRL aperture due to X-ray absorption in the lens material (attenuation length in Al is ~ 0.106 mm at 8.9 keV photon energy). For 23 keV UR (middle and lower plots), a limiting factor is also the size of the UR central cone, since the lens transmits the UR wavefront with only a small “shrinking” (attenuation length of Al is ~ 1.89 mm at 23 keV). The calculations illustrated by Fig. 2 were done using the SRW code [4].

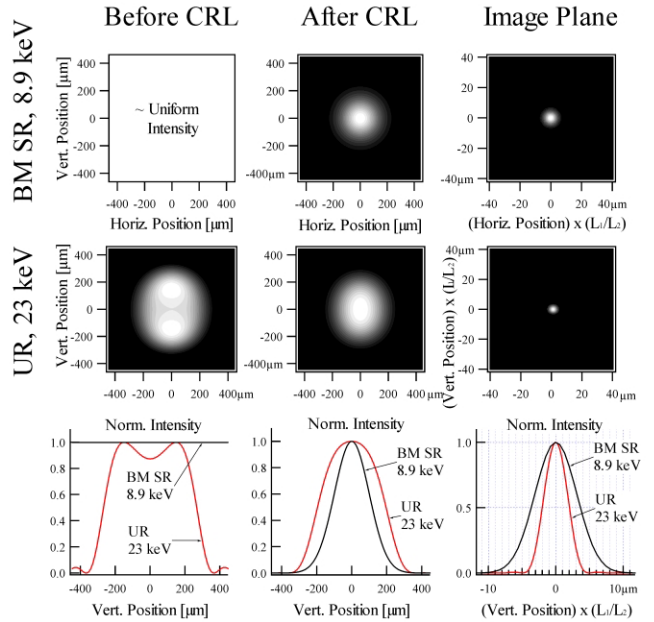


Figure 2. Computed intensity distributions of radiation emitted by one electron and focused by parabolic Al CRLs for two different cases of emission. Lower plots show the vertical cuts of the computed distributions, normalized by the maximum intensity. The horizontal and vertical positions in the image-plane plots (right) are scaled by the de-magnification factor, to show the distributions as for 1:1 imaging.

4 EXPERIMENTAL RESULTS

The detection method used at the BM-5 bending-magnet beamline yields a full 2d intensity distribution in the image plane. We note that the pinhole aperture of 5 μm that limits the spatial resolution of the detector system is of the same order as the spread of the single-electron intensity distribution as calculated in section 3.

Fig. 3 (upper image) shows the full image of the source from the mesh data. Horizontal and vertical cross-sections of this image (lower graphs) reveal that the horizontal and vertical dimensions of the image are in good agreement with published values of the electron beam sizes at a ESRF bending magnet [3].

The detection method used for the measurements at the undulator beamline ID-18 only yields the projections of the 2d intensity distribution on the scanning direction of the fluorescent edge. Fig. 4 shows the horizontal and vertical profiles obtained. Taking into account the demagnification of the X-ray image introduced by the geometry of the setup, the source size comes out to be $907 \times 59 \mu\text{m}^2$ (H×V FWHM). Compared to the literature values of $930 \times 23 \mu\text{m}^2$, there is good agreement for the horizontal size, but a considerable discrepancy for the vertical size value.

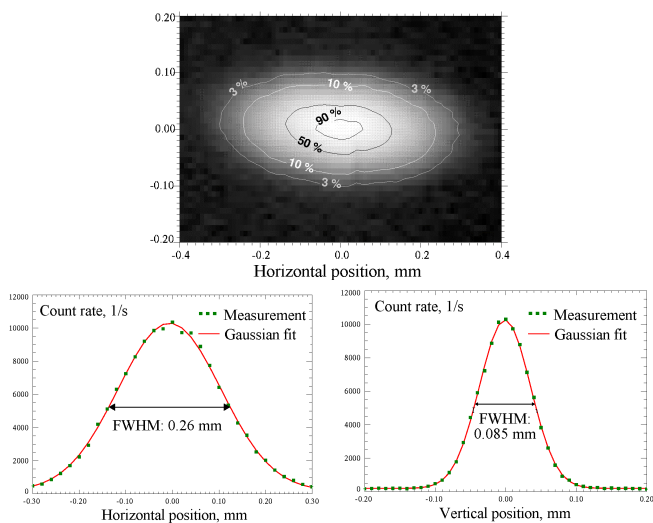


Figure 3. Image of the bending-magnet source at the beamline BM-5, taken at a photon energy of $E = 8.9 \text{ keV}$ with the setup described in the text (upper plot); and horizontal (left) and vertical (right) sections through the center of the image above, fitted with a Gaussian beam. Data of October 1998.

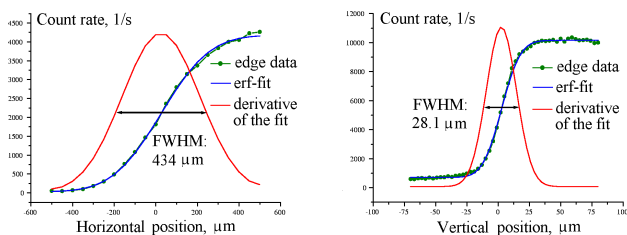


Figure 4. Horizontal (left) and vertical (right) beam profile at the undulator beamline ID-18. Due to the geometry of the imaging setup, the profiles are demagnified by a factor of 2.09. Data of June 1999.

The resolution of the CRL computed in the assumption of perfect parabolic focusing surface (see section 3) is far better than the observed deviation. One of possible reasons for this discrepancy can be the double-crystal Si-111 monochromator that was used to select the photon energy. Slight oscillations of the crystal support as well as a genuine crystal optical effect may explain the result. Another reason for the discrepancy could be a possible small tilt of the electron beam profile in transverse plane with respect to the knife edge. Due to the integration over the large horizontal dimension of the electron beam, a $\sim 20 \text{ mrad}$ tilt could result in the measured value of the vertical size.

5 CONCLUSIONS

The two experiments presented here show that the electron beam imaging in high-energy synchrotron radiation sources using parabolic aluminium compound refractive lenses (CRLs) is a straightforward method of optical diagnostics. Calculations of the transfer function show that the intrinsic optical resolution of such a system is on the order of 5 micrometers. The question of how X-ray crystal monochromator in the beam path influences the imaging properties and the measured source size is yet to be investigated.

The main assets of the method lie firstly in the relative simplicity and mobility of the imaging setup, which is easy to install and align. It can therefore be used at any hard X-ray SR beamline for characterization purposes and without the installation of costly permanent equipment. The only major requirement is that the beamline geometry should allow access to the X-ray beam at two longitudinal positions at reasonably large distances from the source. The method does not interfere with the electron beam. Finally, CRLs can take high intensity and heat load, which make them suitable for optical diagnostics in future light sources.

REFERENCES

- [1] A.Snigirev, V.Kohn, I.Snigireva, B.Lengeler, "A compound refractive lens for focusing high-energy X-rays", *Nature*, 1996, vol.384, p.49.
- [2] B.Lengeler, C.Schroer, M.Richwin, J.Tümmeler, M.Drakopoulos, A.Snigirev and I.Snigireva, *Appl. Phys. Lett.*, vol. 74, 1999, p.3924.
- [3] P.Elleaume, <http://www.esrf.fr/machine/support/ids/Public/Sizes/sizes.html> (as of June 2000)
- [4] O.Chubar, P.Elleaume, "Accurate and efficient computation of synchrotron radiation in the near field region", *Proc. of EPAC-98*, p.1177.